

Laser Printing Single Gold Nanoparticles

Alexander S. Urban,[†] Andrey A. Lutich,^{*†} Fernando D. Stefani,^{*†,‡} and Jochen Feldmann^{*†}

[†]Photonics and Optoelectronics Group, Fakultät für Physik and CeNS, Ludwig-Maximilians-Universität, 80799 Munich, Germany, and [‡]Departamento de Física & Instituto de Física de Buenos Aires (IFIBA, CONICET), Facultad de Ciencias Exactas y Naturales, Universidad de Buenos Aires, Pabellon I Ciudad Universitaria, 1428 Buenos Aires, Argentina

ABSTRACT Current colloidal synthesis is able to produce an extensive spectrum of nanoparticles with unique optoelectronic, magnetic, and catalytic properties. In order to exploit them in nanoscale devices, flexible methods are needed for the controlled integration of nanoparticles on surfaces with few-nanometer precision. Current technologies usually involve a combination of molecular self-assembly with surface patterning by diverse lithographic methods like UV, dip-pen, or microcontact printing.^{1,2} Here we demonstrate the direct laser printing of individual colloidal nanoparticles by using optical forces for positioning and the van der Waals attraction for binding them to the substrate. As a proof-of-concept, we print single spherical gold nanoparticles with a positioning precision of 50 nm. By analyzing the printing mechanism, we identify the key physical parameters controlling the method, which has the potential for the production of nanoscale devices and circuits with distinct nanoparticles.

KEYWORDS Gold nanoparticle, patterning, optical force, nanocircuit, nanopatterning, directed assembly, single nanoparticle

Analogous to combinatorial chemistry methods used in the pharmaceutical industry, high through-put robotized methods have recently begun to be used to explore new nanomaterials.^{3,4} This will enable the production of colloidal nanoparticles (NPs) with properties specifically tailored to specific applications in the near future. The next challenge on the way toward the production of nanoscale devices capitalizing on these properties is the uncomplicated integration of colloidal NPs onto substrates, where they could be connected to, e.g., other NPs, electrodes, or waveguides with a precision of a few nanometers. A number of hybrid lithographical methods have been developed for the arrangement of NPs on surfaces. However, these methods typically involve multiple steps for the chemical patterning of the substrate surface^{2,5,6} and only in special cases provide the capability of immobilizing individual NPs.^{1,7,8} We present a simple method for printing individual NPs directly from the colloidal suspension onto precise positions of a substrate. The method is of general applicability, since the NPs are manipulated by optical forces and the immobilization occurs due to the van der Waals interaction of the NPs with the substrate surface.

To demonstrate this method, we use spherical gold NPs with a diameter of 80 nm, stabilized in colloidal suspension by a coating of CTAB molecules. These constitute an archetypal example of colloidal NPs, which have found numerous applications due to their plasmon resonance at optical frequencies.^{9–12} The NP solution is dropped onto a substrate, which is placed on the scanning stage

of an optical microscope with dark-field illumination, enabling the detection of individual gold NPs (Figure 1a). In addition, the optical microscope is adapted to include a laser beam which is focused on the sample plane and thereby able to apply optical forces on the NPs so as to capture them from the colloidal suspension and push them against the substrate (Figure 1b). In order to avoid spontaneous binding of NPs to the substrate, both should have a net surface charge of equal polarity. The CTAB-coated NPs have a positive surface charge; we thus functionalize the substrates with a layer of the cationic polyelectrolyte PDADMAC (see Supporting Information for details). Therefore, the total interaction between the NPs and the substrate is given by the sum of the electrostatic repulsion ($F_{\text{elect}}(z)$) and the Lifshitz–van der Waals ($F_{\text{LvdW}}(z)$) attraction and can be accounted for with the classic Derjaguin–Landau–Verwey–Overbeek (DLVO) formalism⁸ by differentiating the interaction energies between a charged sphere and a charged surface²¹ to obtain

$$F_{\text{elect}}(z) = \pi\epsilon r \kappa (\zeta_{\text{surf}}^2 + \zeta_{\text{part}}^2 - 2\zeta_{\text{surf}}\zeta_{\text{part}}e^{z\kappa})(\cot(z\kappa) - 1)$$

$$F_{\text{LvdW}}(z) = \frac{2Ar^3}{3z^2(z + 2r)^2}$$

where z is the distance from the surface, r is the particle radius, ζ is the zeta potential, ϵ is the permittivity of the medium, A is the Hamaker constant, and κ^{-1} is the thickness of the electric double layer. The calculated $F_{\text{elect}}(z)$, $F_{\text{LvdW}}(z)$ and total force are shown in Figure 1c for typical experimental conditions used for printing: $\zeta_{\text{part}} =$

* To whom correspondence should be addressed, (F.D.S.) fernando.stefani@df.uba.ar, (A.A.L.) andrey.lutich@physik.lmu.de, or (J.F.) jochen.feldmann@lmu.de.

Received for review: 08/27/2010

Published on Web: 10/19/2010

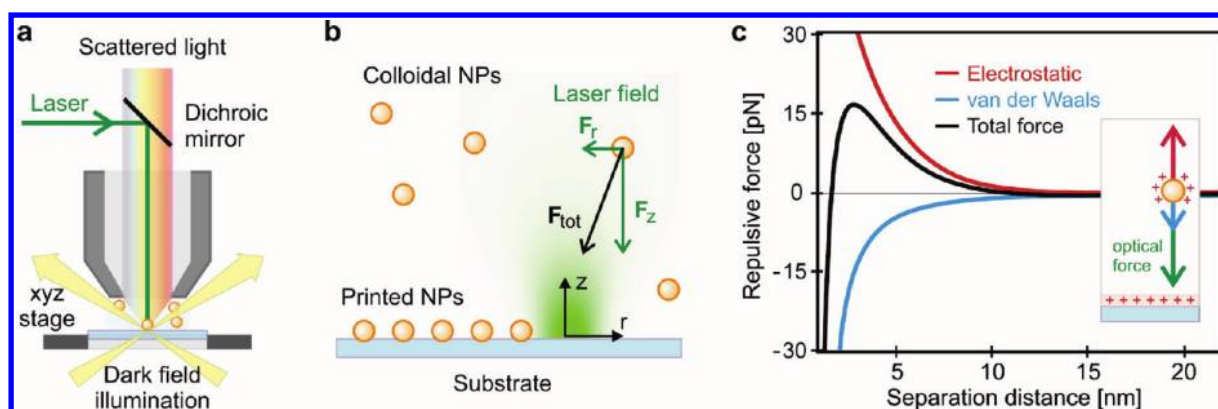


FIGURE 1. Employing optical forces to overcome electrostatic repulsion. (a) Diagram of the experimental setup. A microscope with dark field illumination via an oil immersion condenser (Zeiss Axiotech 100) was adapted to include the manipulation laser (Millenia Vs 532 nm, Spectra-Physics). A $100\times$ (NA 0.9) water immersion objective was used to simultaneously collect scattered light and focus the manipulation laser on the sample. The sample position was controlled with piezo-driven stepper motor translation stages (Linos). Images were acquired using a digital camera (Canon EOS 550D). (b) Schematic representation of the optical forces acting on a NP during the deposition process. (c) Calculated dependence on distance of the electrostatic, van der Waals, and total forces acting on a positively charged Au NP in the vicinity of the positively charged silica surface (for details see Methods) Inset: in order to print the NPs, the optical forces need to surpass the net repulsion.

+30 mV, $\zeta_{\text{surf}} = +30$ mV, $A = 2.5 \times 10^{-20}$, $\kappa^{-1} = 2.2$ nm. Effectively, the electrostatic repulsion forms a potential barrier for the NPs, which they cannot spontaneously overcome. Nonetheless, if the optical forces pushing the NPs against the substrate are sufficiently strong, the NPs may overcome the barrier, coming into close contact with the substrate and remaining immobilized due to the van der Waals interaction (Figure 1c inset).

Since the pioneering work by Ashkin and co-workers,⁹ the optical forces acting on dielectric colloidal particles in a tightly focused laser beam have attracted enormous attention due to their relevance for optical trapping or “tweezing”. Optical forces on metallic NPs have been investigated for trapping, both at wavelengths far from^{11,15} and, more recently, near the plasmon resonances where one has the advantage of an enhanced interaction with light.^{13–15} In our case, we do not use optical forces for trapping but for applying controlled amounts of momentum to the NPs. In Figure 2a the calculated absolute values of the radial (F_r) and axial (F_z) forces acting on an 80 nm gold NP are shown as a function of the position in a Gaussian beam with $\lambda = 532$ nm and a spot size of 380 nm (FWHM) (see Supporting Information for further details). For clarity, only the half-space before the focal plane is shown in Figure 2a; after the focal plane the radial forces change sign, effectively expelling the NPs from the focus. Thus in the experiments we focused the printing beam slightly below the substrate. By equating the maximum force in the axial direction to the force necessary for printing—i.e., the force necessary to overcome the electrostatic barrier according to the DLVO theory (Figure 2)—one obtains an estimated minimum printing laser power of 10 mW. A NP entering the region illuminated by the laser beam is drawn toward the beam center by the radial force and pushed down toward the substrate

by the axial force. Because both forces decrease rapidly with increasing distance from their maxima, only those NPs approaching the proximity of the focal volume will experience forces strong enough to overcome the Brownian motion in order to be guided, surpass the electrostatic barrier, and finally reach the substrate surface. Since the optical forces are directly proportional to E^2 , the volume from which NPs can be captured from the suspension and printed on the substrate can be adjusted simply by regulating the laser power.

In a first experiment, we increase the laser intensity gradually and corroborate that above a certain level NPs are rapidly captured from the suspension and printed onto the substrate. Since the printing process is monitored in real time, single NPs can be printed easily one at a time to form arbitrary patterns. The laser is focused onto a spot slightly below the substrate surface until a NP is printed; the substrate is then displaced in the radial direction and the process is repeated. Figure 2b shows two sample patterns made of individual gold NPs. The binding of the NPs to the substrate is highly stable. Printed NPs resist multiple harsh cleaning and fluid exchanges during which no other NPs attach to the substrate due to the electrostatic repulsion.

To assess the precision of the printing process and the factors affecting it, NPs were printed along lines (Figure 3a), their positions determined via a 2D Gaussian fit of the images (Figure 3b) and statistics computed on their final positions. As a measure for the printing precision, we compute the average deviation from the target line (s , Figure 3b). The larger variations in the interparticle distance are due to the limited accuracy of the transverse positioning stage of our microscope and thus do not contain information on the printing mechanism. Increasing the laser power decreases the precision dramatically;

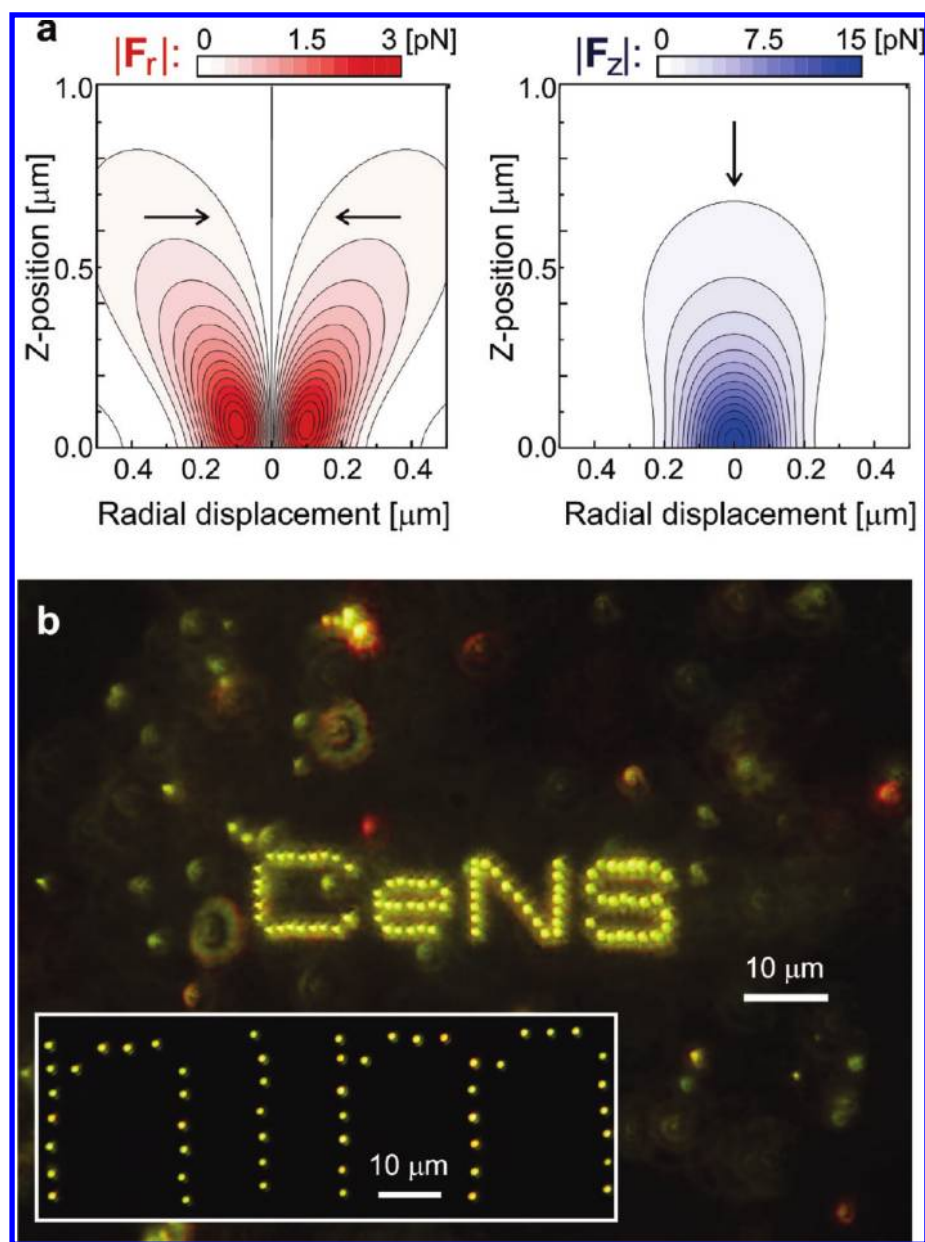


FIGURE 2. Printing individual gold nanoparticles (Au NPs) using optical forces. (a) Calculated radial (left) and axial (right) optical forces acting on an Au NP with a diameter of 80 nm as a function of the position in a Gaussian focused beam (532 nm, 10 mW). The arrows indicate the force directions (see Methods for details). (b) A dark-field image of two patterns made by printing single Au NPs. Each bright green spot within the “CeNS” or the “nim” patterns is a single NP. Bright spots around the pattern are individual NPs freely floating in the colloidal suspension.

the average deviation doubles for a laser power increase of 50%. The reason for this is 3-fold: (i) higher laser powers lead to a larger substrate area around the beam center where the axial optical forces are strong enough to overcome the electrostatic barrier and print NPs; (ii) the higher absorption and consequent heating of the NPs leads to a faster diffusion; and (iii) the stronger axial forces propel the NPs more rapidly to the substrate giving the weaker radial forces less time to guide the NPs to the potential minimum at the center of the beam. Although using the minimum laser power needed to overcome the

electrostatic barrier leads to a higher precision, it is accompanied by a reduced NP capture volume and thus an increased time between printing events. The minimum laser power we use is 300 μW which leads to an average printing time of 5 s per NP. This is significantly lower than the 10 mW prediction based on the forces calculated using the DLVO theory (Figures 1c and 2a). However, this theory does not take into account all forces acting in the experiment. More importantly, reliable values for the Hamaker constant for this material system are unknown. Remarkably, even at this relatively high printing rate, a position-

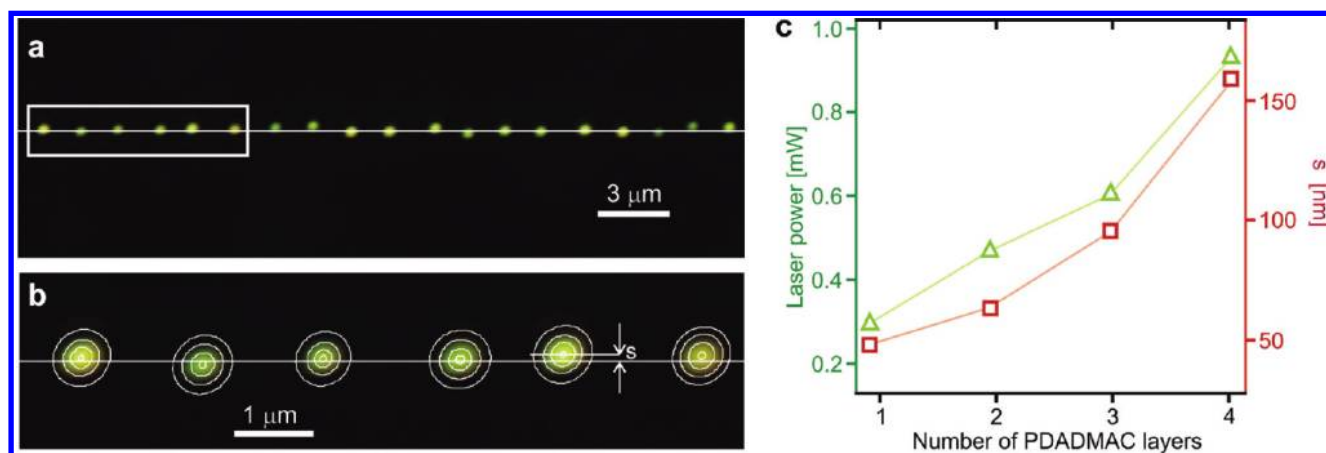


FIGURE 3. Printing precision. (a) A typical dark-field image of a line of printed Au NPs used to estimate printing accuracy. The white line indicates the target line. (b) Detail of the area marked by the rectangle in (a) including the results of the 2D Gaussian fit of each individual NP used to determine NP positions and the printing accuracy s . (c) Minimum laser power needed for efficient printing (5 s/NP; triangles) and printing accuracy (squares) measured for substrates with increasing number of polymer layers. The lines are guides to the eye.

ing precision of 50 nm, roughly half the diameter of the NPs is achieved (Figures 3b,c). Finally, we test the influence of additional polyelectrolyte layers on the substrate. As expected, they constitute an obstacle for the NPs and higher laser powers are required for printing. In turn, those higher laser powers lead to a reduced printing precision (Figure 3c).

In conclusion, we have demonstrated the laser printing of individual gold NPs directly from a colloidal suspension. This new method enables the controlled incorporation of single NPs to specific locations on a substrate with a precision of a few tens of nanometers using laser powers well below 1 mW. The deposition technique relies fully on optical forces to (i) capture the NPs from the colloidal suspension, (ii) guide them toward the printing position, and (iii) overcome the electrostatic repulsion and fix them on the substrate through van der Waals attraction. The printed NPs remain immobilized after repeated steps of drying and rinsing. The simplicity of the method and high degree of control over the deposition parameters make it extremely versatile; higher deposition precision by more accurate sample positioning, control of temperature and viscosity or the incorporation of microinjection are being explored as well as the control of NP orientation using polarized light. Since the concepts presented here for gold NPs are valid and easily extended to other NPs, this laser printing method holds promise for the production of various nanoscale devices and circuits.

Acknowledgment. Financial support by the DFG through the Nanosystems Initiative Munich (NIM) and *LMUexcellent* is gratefully acknowledged. F.D.S. is a CONICET fellow.

Supporting Information Available. Additional information regarding sample preparation and calculation of

optical forces and video showing the printing process. This material is available free of charge via the Internet at <http://pubs.acs.org>.

REFERENCES AND NOTES

- (1) Kraus, T.; et al. Nanoparticle printing with single-particle resolution. *Nat. Nanotechnol.* **2007**, *2*, 570–576.
- (2) Saavedra, H. M.; et al. Hybrid strategies in nanolithography. *Rep. Prog. Phys.* **2010**, *73*, No. 036501.
- (3) Su, G.; Yan, B. Nano-combinatorial chemistry strategy for nanotechnology research. *J. Comb. Chem.* **2010**, *12*, 215–221.
- (4) Chan, E. M.; Xu, C.; Mao, A. W.; Han, G.; Owen, J. S.; Cohen, B. E.; Milliron, D. J. Reproducible, High-Throughput Synthesis of Colloidal Nanocrystals for Optimization in Multidimensional Parameter Space. *Nano Lett.* **2010**, *10*, 1874–1885.
- (5) Hung, A. M.; et al. Large-area spatially ordered arrays of gold nanoparticles directed by lithographically confined DNA origami. *Nat. Nanotechnol.* **2010**, *5*, 121–126.
- (6) Lee, T. I.; Choi, W. J.; Moon, K. J.; Choi, J. H.; Kar, J. P.; Das, S. N.; Kim, Y. S.; Baik, H. K.; Myoung, J. M. Programmable Direct-Printing Nanowire Electronic Components. *Nano Lett.* **2010**, *10*, 1016–1021.
- (7) Shin, C.; et al. Single nanoparticle alignment by atomic force microscopy indentation. *Appl. Phys. Lett.* **2009**, *94*, 163107.
- (8) Hoogenboom, J. P.; et al. Patterning surfaces with colloidal particles using optical tweezers. *Appl. Phys. Lett.* **2002**, *80*, 4828–4830.
- (9) Sönnichsen, C.; et al. A molecular ruler based on plasmon coupling of single gold and silver nanoparticles. *Nat. Biotechnol.* **2005**, *23*, 741–745.
- (10) Wang, H.; Levin, C. S.; Halas, N. J. Nanosphere arrays with controlled sub-10-nm gaps as surface-enhanced raman spectroscopy substrates. *J. Am. Chem. Soc.* **2005**, *127*, 14992–14993.
- (11) Mayilo, S.; Kloster, M. A.; Wunderlich, M.; Lutich, A.; Klar, T. A.; Nichtl, A.; Kürzinger, K.; Stefani, F. D.; Feldmann, J. Long-Range Fluorescence Quenching by Gold Nanoparticles in a Sandwich Immunoassay for Cardiac Troponin T. *Nano Lett.* **2009**, *9*, 4558–4563.
- (12) Urban, A. S.; Fedoruk, M.; Horton, M. R.; Rädler, A. S.; Stefani, F. D.; Feldmann, J. Controlled Nanometric Phase Transitions of Phospholipid Membranes by Plasmonic Heating of Single Gold Nanoparticles. *Nano Lett.* **2009**, *9*, 2905–2908.
- (13) Israelachvili, J. N. *Intermolecular and surface forces*; Elsevier Science: Amsterdam, 1991.
- (14) Ashkin, A. Optical trapping and manipulation of neutral particles using lasers. *Proc. Natl. Acad. Sci. U.S.A.* **1997**, *94*, 4853–4860.

- (15) Svoboda, K.; Block, S. M. Optical trapping of metallic Rayleigh particles. *Opt. Lett.* **1994**, *19*, 930–932.
- (16) Hansen, P. M.; Bhatia, V. K.; Harrit, N.; Oddershede, L. Expanding the Optical Trapping Range of Gold Nanoparticles. *Nano Lett.* **2005**, *5*, 1937–1942.
- (17) Toussaint, K. C.; et al. Plasmon resonance-based optical trapping of single and multiple Au nanoparticles. *Opt. Express* **2007**, *15*, 12017–12029.
- (18) Arias-González, J. R.; Nieto-Vesperinas, M. Optical forces on small particles: attractive and repulsive nature and plasmon-resonance conditions. *J. Opt. Soc. Am. A* **2003**, *20*, 1201–1209.
- (19) Dienerowitz, M.; Mazilu, M.; Dholakia, K. Optical manipulation of nanoparticles: a review. *J. Nanophoton.* **2008**, *2*, No. 021875.
- (20) Caruso, F.; Lichtenfeld, H.; Donath, E.; Möhwald, H. Investigation of Electrostatic Interactions in Polyelectrolyte Multilayer Films: Binding of Anionic Fluorescent Probes to Layers Assembled onto Colloids. *Macromolecules* **1999**, *32*, 2317–2328.
- (21) Bos, R.; van Der Mei, H. C.; Busscher, H. J. Physico-chemistry of initial microbial adhesive interactions—its mechanisms and methods for study. *FEMS Microbiol. Rev.* **1999**, *23*, 179–230.
- (22) Agayan, R. R.; et al. Optical trapping near resonance absorption. *Appl. Opt.* **2002**, *41*, 2318–2327.